

Tổng hợp vật liệu composite g-C₃N₄/ZnO tăng cường hoạt tính quang xúc tác dưới ánh sáng nhìn thấy

Phan Thị Thùy Trang^{1,*}, Đặng Trung Hậu², Nguyễn Vũ Diệu Linh²,
Nguyễn Văn Thưởng², Nguyễn Hồ Duy², Nguyễn Lương Khương An²,
Mai Thị Tường Vy³, Nguyễn Thị Lan^{1,*}

¹Khoa Khoa học Tự nhiên, Trường Đại học Quy Nhơn, Việt Nam

²Khoa Sư Phạm, Trường Đại học Quy Nhơn, Việt Nam

³Phòng Hành chính - Tổng hợp, Trường Đại học Quy Nhơn, Việt Nam

Ngày nhận bài: 03/12/2023; Ngày sửa bài: 07/03/2024;

Ngày nhận đăng: 25/03/2024; Ngày xuất bản: 28/06/2024

TÓM TẮT

Vật liệu composite ZnO/g-C₃N₄ đã được tổng hợp thành công bằng phương pháp nung đơn giản từ các tiền chất g-C₃N₄ và zinc acetate hexahydrate. Hình thái, độ kết tinh, thuộc tính hình học và liên kết hóa học của vật liệu được đặc trưng bằng các kỹ thuật phân tích khác nhau như hiển vi điện tử quét (SEM), nhiễu xạ tia X (XRD), phổ phản xạ khuếch tán tử ngoại khả kiến (UV-Vis DRS), phổ hồng ngoại (FT-IR). Vật liệu được đánh giá hiệu quả quang xúc tác qua phản ứng phân hủy dung dịch rhodamine B (RhB) dưới ánh sáng nhìn thấy. Kết quả cho thấy hoạt tính quang xúc tác của vật liệu composite phân hủy dung dịch RhB cao hơn các vật liệu đơn ZnO, g-C₃N₄ với hằng số tốc độ phản ứng phân hủy là 0.0243 phút⁻¹, gấp hơn hai lần so với g-C₃N₄ tinh khiết (0.0091 phút⁻¹).

Từ khóa: g-C₃N₄, ZnO, composite, hoạt tính quang xúc tác, rhodamine B.

*Tác giả liên hệ chính.

Email: nguyenthilan@qnu.edu.vn, phanthithuytrang@qnu.edu.vn

Synthesis of g-C₃N₄/ZnO composite with enhanced visible light photocatalytic activity

Phan Thi Thuy Trang^{1,*}, Dang Trung Hau², Nguyen Vu Dieu Linh²,
Nguyen Van Thuong², Nguyen Ho Duy², Nguyen Luong Khuong An²,
Mai Thi Tuong Vy³, Nguyen Thi Lan^{1,*}

¹*Faculty of Natural Sciences, Quy Nhon University, Vietnam*

²*Faculty of Education, Quy Nhon University, Vietnam*

³*Administrative - General Office, Quy Nhon University, Vietnam*

Received: 03/12/2023; Revised: 07/03/2024;

Accepted: 25/03/2024; Published: 28/06/2024

ABSTRACT

ZnO/g-C₃N₄ composite material was successfully synthesized using a facile calcination method with g-C₃N₄ and zinc acetate hexahydrate as the precursors. The morphology, crystallinity, optical properties, and chemical bond characteristics of the synthesized composite were characterized by using various analytical techniques such as scanning electron microscopy (SEM), Fourier-transform infrared (FTIR) spectroscopy, X-ray powder diffraction (XRD), ultraviolet-visible diffuse reflectance spectroscopy (UV-Vis DRS). The material's photocatalytic performance was evaluated through the decomposition of rhodamine B (RhB) solution under visible light. The results show that the photocatalytic properties of composite materials decomposing RhB dye solution are higher than those of single materials ZnO, g-C₃N₄ with a decomposition reaction rate constant of 0.0243 min⁻¹, more than twice as fast compared to pure g-C₃N₄ (0.0091 min⁻¹).

Keywords: g-C₃N₄, ZnO, composite, photocatalytic activity, rhodamine B.

1. INTRODUCTION

Along with economic development nowadays, the problem of environmental pollution is becoming increasingly serious. Therefore, effectively treating ecological decay is a challenging problem at the global level. Environmental treatment methods have been widely researched and have achieved many good results, including popular methods such as physics, chemistry, and biology. Recently, an attractive method for scientists to treat difficult-to-decompose organic substances is using semiconductor photocatalytic

materials. Among the semiconductors published to date, metal oxides are the most studied due to their chemical and photochemical stability, low toxicity, and low cost.¹ Among the oxides, TiO₂ and ZnO are of most interest.² ZnO is a potential candidate for photocatalytic reactions due to its high photocatalytic activity, environmental compatibility, and relatively low cost and is therefore widely used in wastewater treatment.^{3,4}

Zinc oxide (ZnO) is a widely researched and widely used semiconductor in photocatalysis. However, ZnO has a wide band gap energy (about

*Corresponding author:

Email: nguyenthilan@qnu.edu.vn, phanthithuytrang@qnu.edu.vn

3.37 eV), so it is less active in the visible light region.⁵ It is an exciting idea to prepare a mix with two photocatalysts by appropriate matching band-level sites to reduce the electron–hole pair recombination.⁶

Recently, $\text{g-C}_3\text{N}_4$ material, a polymer organic semiconductor with a graphitic-like structure, can absorb visible light (the band gap energy of about 2.7 eV), taking many interest researchers due to its wide range of applications. However, the fast recombination rate of photoinduced electron-hole pair for this material leads to its low photoefficiency. This is a drawback when using it in individual status. Therefore, many attempts to enhance the photocatalytic performance of $\text{g-C}_3\text{N}_4$ by modifying it with other elements have been made.^{7,8}

In this study, the $\text{ZnO/g-C}_3\text{N}_4$ composite was synthesized by a simple calcination method, and its photocatalytic efficiency was determined through the degradation of RhB under visible light.

2. EXPERIMENTAL

2.1. Material synthesis

Chemicals

All the chemicals for materials synthesis, including *zinc acetate* dehydrate $\text{Zn}(\text{CH}_3\text{COO})_2 \cdot 2\text{H}_2\text{O}$ (99.5%), urea $(\text{CO}(\text{NH}_2)_2, \geq 99\%)$, rhodamine B ($\text{C}_{28}\text{H}_{31}\text{ClN}_2\text{O}_3$) were purchased from Merck.

Synthesis

The pure $\text{g-C}_3\text{N}_4$ was prepared by heating urea in an alumina crucible covered by an alumina sealed with aluminum foil at 550 °C in the Argon gas for an hour with a temperature ramping of 10 °C·min⁻¹. The obtained solid product was reground and denoted as $\text{g-C}_3\text{N}_4$.

The $\text{g-C}_3\text{N}_4/\text{ZnO}$ was synthesized through the calcination facile method. Firstly, 100 mg of $\text{g-C}_3\text{N}_4$ was a mixture with 200 mg of zinc acetate dehydrate $\text{Zn}(\text{CH}_3\text{COO})_2 \cdot 2\text{H}_2\text{O}$. Next, the mixture was ground finely and calcined in the air at 350 °C for 1 hour. The solid was

filtered, washed, and dried at 80 °C for 24 hours to obtain the composite product $\text{ZnO/g-C}_3\text{N}_4$ (denoted as ZCN). ZnO was also synthesized similarly to the above conditions but without $\text{g-C}_3\text{N}_4$ (marked as ZnO).

2.2. Characterization

Powder X-ray diffraction (PXRD) patterns were acquired using a Bruker diffractometer (D/max 2200) with Ni-filtered Cu Ka radiation ($\text{k} = 1.5418 \text{ \AA}$), power 40 kV, current 40 mA. Scanning angle from 10 to 80°. The Fourier-transform infrared (FT-IR) spectroscopy was carried out on an IRAffinity-1S spectrometer (Shimadzu) with wavenumbers ranging from 400 to 4000 cm^{-1} . The composition of the element was determined by EDS spectroscopy. UV-Vis-DRS spectra of material samples were determined on a Jasco-V770 machine with wavelengths from 200 - 800 nm. The morphology and size of the synthesized samples were characterized by scanning electron microscopy (SEM, JEOL JSM-600F).

2.3. Photocatalytic properties

Rhodamine B (RhB, $\text{C}_{28}\text{H}_{31}\text{ClN}_2\text{O}_3$) was selected as an organic pollutant to evaluate photocatalytic activity. To 100 mL of 10 mg/L RhB solution, 0.05 g of prepared sample was dispersed under stirring, and the solution was kept in a dark condition for 30 min. Then, the solution was irradiated by visible light using a 30 W LED lamp source. RhB degradation was monitored by taking suspension at irradiation time intervals of 20 min. Each suspension was centrifuged to separate the catalyst from the RhB solution. Subsequently, the degradation rate was calculated as a function of irradiation time from the change in absorbance at a wavelength of 553 nm as measured using a UV-Vis spectrophotometer (Jenway 6800).

3. RESULTS AND DISCUSSION

3.1. Material characteristics

The X-ray diffraction patterns of ZnO , $\text{g-C}_3\text{N}_4$, and ZCN composite are shown in Figure 1. The

patterns show that the photocatalysts are well crystallized, the pure $\text{g-C}_3\text{N}_4$ sample has two distinct peaks at 12.87° and 27.69° , which are indexed for graphitic materials as the (100) and (002).⁹ The peak at 12.87° represents stacking of aromatic units corresponding to the interplanar distance of 6.82 \AA . The strong peak at 27.69° is interlayer packing of aromatic tri-s-triazine with a stacking distance of 3.22 \AA .¹⁰ Meanwhile, the diffraction peaks at $20 = 31.76^\circ$, 34.44° , 36.26° , 47.56° , 56.64° , 62.94° và 68.19° in XRD patterns of ZnO , corresponding to the (100), (002), (101), (102), (110), (103) and (112).¹¹ The XRD peaks of the pure ZnO sample agree with the hexagonal wurtzite structure (JCPDS No. 001-1136). The locus and shapes of characteristic peaks of ZCN are unchanged compared with those of pure ZnO . This demonstrated that modification with $\text{g-C}_3\text{N}_4$ does not affect ZnO 's lattice structure, which is suitable for photocatalytic properties of as-prepared hybrid photocatalysts. As for a combination, the ZCN composites show the X-ray patterns analogous to the X-ray patterns of the components. The diffraction peaks of both ZnO and $\text{g-C}_3\text{N}_4$ phases are observable.

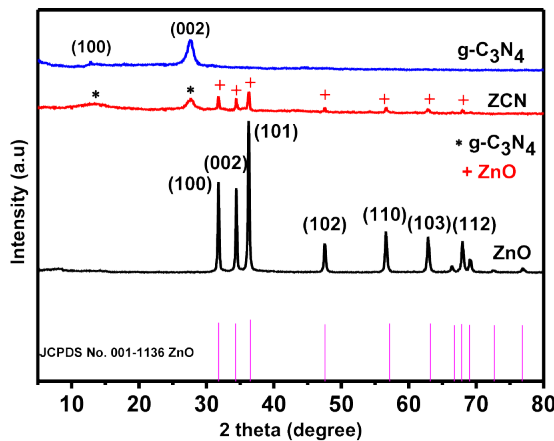


Figure 1. XRD patterns of $\text{g-C}_3\text{N}_4$, ZnO , and ZCN.

The bond structure of ZnO , $\text{g-C}_3\text{N}_4$, and ZCN composite were analyzed by FT-IR measurement. Figure 2 shows that the spectrum of $\text{g-C}_3\text{N}_4$ has found some strong bands in the $1616 - 1200 \text{ cm}^{-1}$ range, corresponding to typical stretching vibrations of C-N, C = N heterocycles.¹² The peak at 800 cm^{-1} was assigned

to the s-triazine ring vibrations. While the peaks at 1616 , 1560 , 1461 , and 1405 cm^{-1} were ascribed to stretching vibrations of heptazine-desired repeating units. The peak at 1313 and 1232 cm^{-1} belonged to the stretching vibration of connected trigonal units of C-N(-C)-C of bridging C-NH-C (partial condensation).¹³ Meanwhile, the broad absorption band $3300 - 3000 \text{ cm}^{-1}$ and a small peak at 891 cm^{-1} can be ascribed to the N-H stretching vibrations and bend vibration, respectively.¹⁴⁻¹⁷ With the ZnO sample, there was a Zn-O bond vibration band at $550-450 \text{ cm}^{-1}$.¹⁸ In general, all the characteristic peaks of ZnO and $\text{g-C}_3\text{N}_4$ appeared in the spectra of ZCN. Combined with the XRD and FT-IR analysis, it reconfirmed the successful synthesis of the ZCN composite. The result showed a strong interaction between $\text{g-C}_3\text{N}_4$ and ZnO semiconductors.

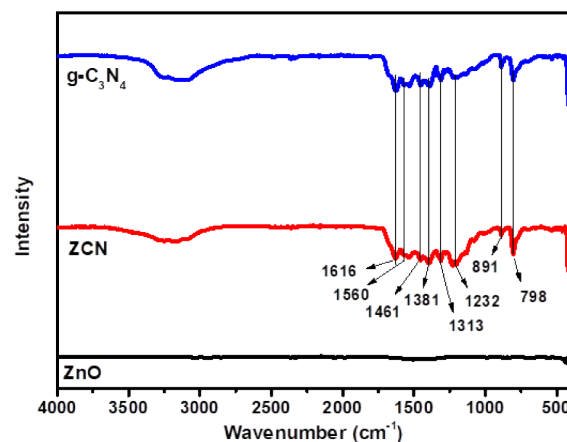


Figure 2. IR spectra of ZnO , $\text{g-C}_3\text{N}_4$ and ZCN.

The morphologies of ZnO , $\text{g-C}_3\text{N}_4$, and ZCN samples are indicated through SEM images in Figure 3.

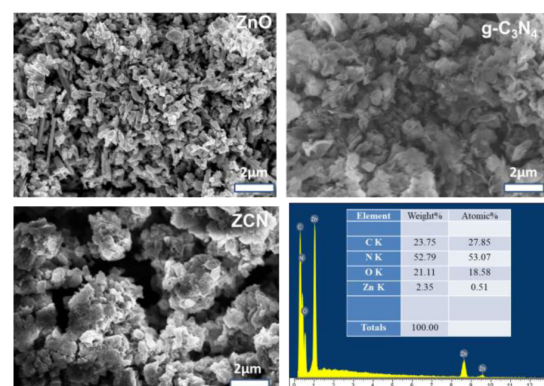


Figure 3. FE-SEM images of ZnO , $\text{g-C}_3\text{N}_4$, ZCN, and EDS image of ZCN.

The results show that a typical multi-layered structure of graphitic carbon nitride corresponds to the in-plane structural packing pattern of tri-s-triazine building blocks. Figure 3 indicates that the ZCN material has micropores with large diameters. SEM image of ZnO in uneven sheet form, flat surface. After combining with $\text{g-C}_3\text{N}_4$, the morphology of ZCN changed significantly. This change in morphology can be ascribed to the surface deposition of $\text{g-C}_3\text{N}_4$ on the ZnO. The thin nanosheets encircled ZnO can be ascribed to $\text{g-C}_3\text{N}_4$ nanosheets. The ZnO core was uniformly beset with thin $\text{g-C}_3\text{N}_4$ flakes.¹⁴ These results further confirm the successful formation of the heterostructure of ZCN. Figure 3 shows enough presence of elements Zn, O, C, and N in a composite sample of the EDS spectrum.

UV-vis diffuse reflectance spectra investigated optical absorptions of $\text{g-C}_3\text{N}_4$, ZnO, and ZCN (Figure 4).

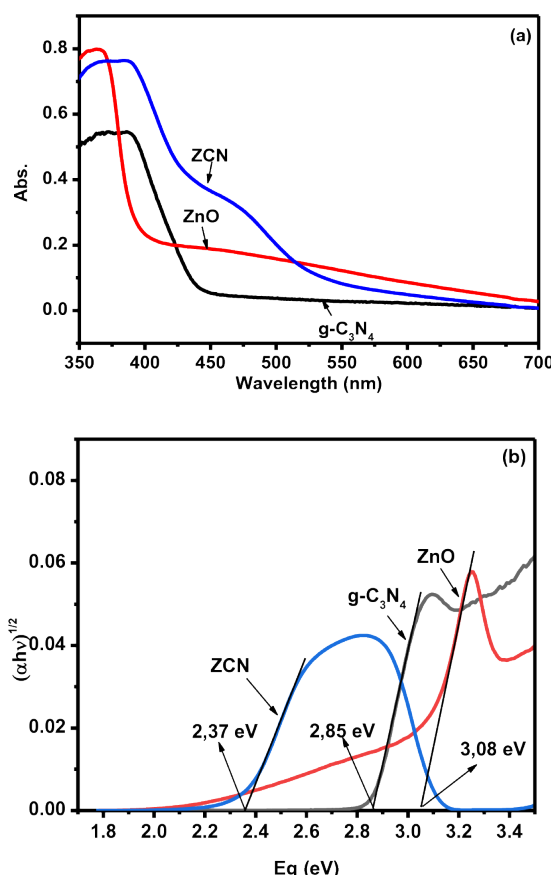


Figure 4. UV-Vis-DRS (a) and band gap of ZnO, $\text{g-C}_3\text{N}_4$, and ZCN (b).

The results show a clear fundamental absorption edge of ZnO at 395 nm, and the band gap energy is determined to be 3.08 eV. Meanwhile, the main absorption edge of pure $\text{g-C}_3\text{N}_4$ occurs at a wavelength of about 445 nm and a band gap energy of 2.85 eV. As expected, compared with pure ZnO, the ZCN photocatalyst shows the same absorption edge, but the absorption extends to the visible light in the presence of $\text{g-C}_3\text{N}_4$. This result can be expected to be that the photocatalytic reaction of ZnO is improved under visible light irradiation when $\text{g-C}_3\text{N}_4$ is introduced into ZnO and leads to charge transfer between $\text{g-C}_3\text{N}_4$ and the valence band of ZnO.

3.2. Photocatalytic properties of materials

The photocatalytic activity of the decomposition of RhB solution (10 mg/L) by LED lamp 30 W of materials is shown in Figure 5.

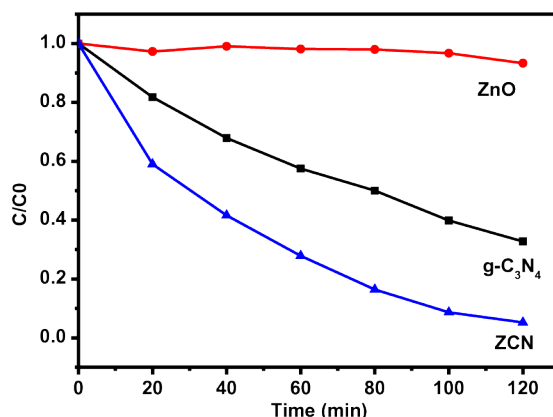


Figure 5. Decolorization kinetics of RhB over ZnO, $\text{g-C}_3\text{N}_4$, and ZCN under visible light irradiation (conditions: $m_{\text{catalyst}} = 0.05$ g; concentration of RhB = 10 mg/L; adsorption time = 30 min).

Before evaluating the catalytic activity, the material samples were adsorbed in the dark for 30 minutes to reach adsorption/desorption equilibrium. Figure 5 shows that the ZCN sample exhibits higher photocatalytic activity to decompose RhB than the single ZnO and $\text{g-C}_3\text{N}_4$ after 120 minutes of illumination. Specifically, the photocatalytic efficiency of samples ZnO, $\text{g-C}_3\text{N}_4$, and ZCN is 6.68%, 67.27%, and 94.75%, respectively, while ZnO has almost

no photocatalytic properties. The improved photocatalytic activity of the composite is due to the synergistic effect of ZnO and g-C₃N₄. The connection of two semiconductors (ZnO and g-C₃N₄) will form a heterojunction at the contact surface. And the formed heterojunctions are beneficial to the effective separation of charge carriers. The presence of g-C₃N₄ in the ZCN sample overcomes the disadvantage of photogenerated electron-hole recombination that occurs in individual semiconductor materials.

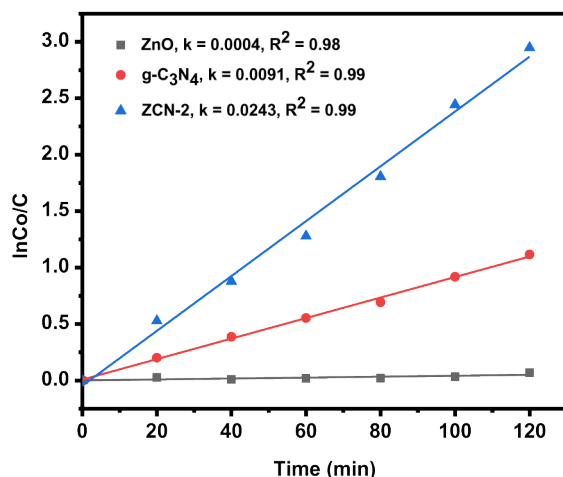


Figure 6. Plot of Langmuir-Hinshelwood model of ZnO, $g\text{-C}_3\text{N}_4$, and ZCN materials.

To investigate the kinetics of photocatalytic reactions, the Langmuir–Hinshelwood model is usually employed (Figure 6). It can be observed that the plots of $\ln(C_0/C)$ versus reaction time (t) are well fit by the pseudo-first-order rate model with high correlation coefficients R^2 (0.99–1).

The results show that the ZCN catalyst has the highest reaction rate (0.0243 min^{-1}), which is 2.76 times higher than $g\text{-C}_3\text{N}_4$, and is much more significant than ZnO material. This result indicates that adding $g\text{-C}_3\text{N}_4$ to ZnO significantly improved the photocatalytic activity of pure ZnO.

4. CONCLUSION

ZCN material is synthesized by a simple calcination method. This heterostructure shows the ability to effectively capture and store charge in the visible light region, significantly improving

the photocatalytic efficiency of the material in the decomposition of RhB in a water environment. The reaction follows a Langmuir–Hinshelwood model with a calculated rate constant of 0.0243 min^{-1} . The ZCN composite material exhibits good heterojunction between ZnO and $g\text{-C}_3\text{N}_4$ and is a promising semiconductor material for decomposing organic dyes in water solution by photocatalysis under visible light.

REFERENCES

1. S. Ahmed, M. Rasul, R. Brown, M. Hashib. Influence of parameters on the heterogeneous photocatalytic degradation of pesticides and phenolic contaminants in wastewater: a short review, *Journal of Environmental Management*, **2011**, 92(3), 311-330.
2. M. Azarang, A. Shuhaimi, R. Yousefi, S. P. Jahromi. One-pot sol–gel synthesis of reduced graphene oxide uniformly decorated zinc oxide nanoparticles in starch environment for highly efficient photodegradation of methylene blue, *RSC Advances*, **2015**, 5(28), 21888-21896.
3. S. M. Jilani, P. Banerji. Graphene oxide–zinc oxide nanocomposite as channel layer for field effect transistors: effect of ZnO loading on field effect transport, *ACS Applied Materials & Interfaces*, **2014**, 6(19), 16941-16948.
4. M. Azarang, A. Shuhaimi, R. Yousefi, A. M. Golsheikh, M. Sookhakian. Synthesis and characterization of ZnO NPs/reduced graphene oxide nanocomposite prepared in gelatin medium as highly efficient photo-degradation of MB, *Ceramics International*, **2014**, 40(7), 10217-10221.
5. X. Huang, C. Tay, Z. Zhan, C. Zhang, L. Zheng, T. Venkatesan, S. Chua. Universal photoluminescence evolution of solution-grown ZnO nanorods with annealing: important role of hydrogen donor, *CrystEngComm*, **2011**, 13(23), 7032-7036.
6. M. H. Suhag, A. Khatun, I. Tateishi, M. Furukawa, H. Katsumata, S. Kaneko. One-step fabrication of the ZnO/ $g\text{-C}_3\text{N}_4$ composite for visible light-responsive photocatalytic

degradation of bisphenol E in aqueous solution, *ACS Omega*, **2023**, 8(13), 11824-11836.

7. S. Stolbov, S. Zuluaga. Sulfur doping effects on the electronic and geometric structures of graphitic carbon nitride photocatalyst: insights from first principles, *Journal of Physics: Condensed Matter*, **2013**, 25(8), 085507.

8. M. Tahir, C. Cao, F. K. Butt, S. Butt, F. Idrees, Z. Ali, I. Aslam, M. Tanveer, A. Mahmood, N. Mahmood. Large scale production of novel $g\text{-C}_3\text{N}_4$ micro strings with high surface area and versatile photodegradation ability, *CrystEngComm*, **2014**, 16(9), 1825-1830.

9. B. Zhu, P. Xia, Y. Li, W. Ho, J. Yu. Fabrication and photocatalytic activity enhanced mechanism of direct Z-scheme $g\text{-C}_3\text{N}_4/\text{Ag}_2\text{WO}_4$ photocatalyst, *Applied Surface Science*, **2017**, 391, 175-183.

10. X. Li, M. Li, J. Yang, X. Li, T. Hu, J. Wang, Y. Sui, X. Wu, L. Kong. Synergistic effect of efficient adsorption $g\text{-C}_3\text{N}_4/\text{ZnO}$ composite for photocatalytic property, *Journal of Physics and Chemistry of Solids*, **2014**, 75(3), 441-446.

11. K. Dulta, G. K. Ağçeli, P. Chauhan, R. Jasrotia, P. Chauhan. Ecofriendly synthesis of zinc oxide nanoparticles by Carica papaya leaf extract and their applications, *Journal of Cluster Science*, **2021**, 1-15.

12. B. V. Lotsch, M. Döblinger, J. Sehnert, L. Seyfarth, J. Senker, O. Oeckler, W. Schnick. Unmasking melon by a complementary approach employing electron diffraction, solid-state NMR spectroscopy, and theoretical calculations-structural characterization of a carbon nitride polymer, *Chemistry-A European Journal*, **2007**, 13(17), 4969-4980.

13. J. Liu, T. Zhang, Z. Wang, G. Dawson, W. Chen. Simple pyrolysis of urea into graphitic carbon nitride with recyclable adsorption and photocatalytic activity, *Journal of Materials Chemistry*, **2011**, 21(38), 14398-14401.

14. N. Nie, L. Zhang, J. Fu, B. Cheng, J. Yu. Self-assembled hierarchical direct Z-scheme $g\text{-C}_3\text{N}_4/\text{ZnO}$ microspheres with enhanced photocatalytic CO_2 reduction performance, *Applied Surface Science*, **2018**, 441, 12-22.

15. C. Xing, Z. Wu, D. Jiang, M. Chen. Hydrothermal synthesis of $\text{In}_2\text{S}_3/g\text{-C}_3\text{N}_4$ heterojunctions with enhanced photocatalytic activity, *Journal of Colloid and Interface Science*, **2014**, 433, 9-15.

16. D. Jiang, L. Chen, J. Zhu, M. Chen, W. Shi, J. Xie. Novel p-n heterojunction photocatalyst constructed by porous graphite-like C_3N_4 and nanostructured BiOI: facile synthesis and enhanced photocatalytic activity, *Dalton Transactions*, **2013**, 42(44), 15726-15734.

17. J. Hong, X. Xia, Y. Wang, R. Xu. Mesoporous carbon nitride with in situ sulfur doping for enhanced photocatalytic hydrogen evolution from water under visible light, *Journal of Materials Chemistry*, **2012**, 22(30), 15006-15012.

18. D. R. Paul, S. Gautam, P. Panchal, S. P. Nehra, P. Choudhary, A. Sharma. ZnO -modified $g\text{-C}_3\text{N}_4$: a potential photocatalyst for environmental application, *ACS Omega*, **2020**, 5(8), 3828-3838.



Copyright © The Author(s) 2024. This work is licensed under the Creative Commons Attribution-NonCommercial 4.0 International License.